ACS central science

Research Article

http://pubs.acs.org/journal/acscii

A General Small-Scale Reactor To Enable Standardization and Acceleration of Photocatalytic Reactions

Chi "Chip" Le,[†,‡] Michael K. Wismer,[‡,§] Zhi-Cai Shi,[‡,§] Rui Zhang,[§] Donald V. Conway,[§] Guoqing Li,[§] Petr Vachal,[§] Ian W. Davies,[*,§] and David W. C. MacMillan[*,†]

[†]Merck Center for Catalysis at Princeton University, Princeton, New Jersey 08544, United States

[§]Discovery Chemistry and Process Research & Development, Merck & Co., Inc., Kenilworth, New Jersey 07033, United States

Supporting Information

ABSTRACT: Photocatalysis for organic synthesis has experienced an exponential growth in the past 10 years. However, the variety of experimental procedures that have been reported to perform photon-based catalyst excitation has hampered the establishment of general protocols to convert visible light into chemical energy. To address this issue, we have designed an integrated photoreactor for enhanced photon capture and catalyst excitation. Moreover, the evaluation of this new reactor in eight photocatalytic transformations that are widely employed in medicinal chemistry settings has confirmed significant performance advantages of this optimized design while enabling a standardized protocol.

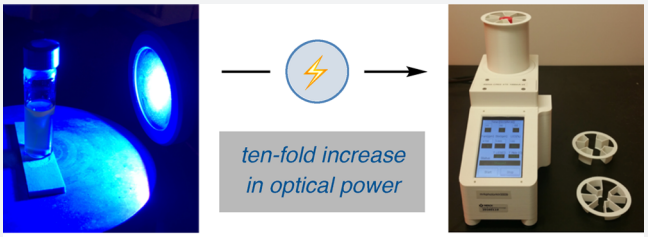

Standardization and Acceleration of Photocatalytic Reactions

INTRODUCTION

The utilization of photon-harvesting molecules to convert visible light to chemical energy, known as photocatalysis, has long been a key technology in many important processes such as water splitting,[1,2] CO_2 reduction,[3] and solar energy capture.[4] Recently, however, the application of visible-light photoredox catalysis to synthetic organic chemistry has become an area of significant interest.[5] Indeed, over the past 10 years there has been an exponential growth in the number of photocatalysis studies that have been reported in the organic literature.[6] Among several important features, the ability of photoredox catalysts to generate open-shell organic species in a controlled and selective fashion has enabled the invention of a myriad of powerful technologies for bond construction.[7,8] Moreover, the merger of photoredox catalysis with additional modes of catalytic activation (e.g., transition metal catalysis, organocatalysis) has led to unanticipated breakthroughs in the development of fragment-coupling reactions of value to medicinal and process chemistry.[9]

The utilization of visible and UVA light and the commoditization of low-cost high-energy LEDs has enabled photoredox catalysis to be quickly deployed in both academic and industrial settings. While broad focus has been placed on the goal of new reaction invention, there has also been significant interest in improving the rates of these newly discovered photon-mediated reactions while developing standardized operating protocols. The Beer–Lambert law dictates that the photonic flux decreases exponentially with depth in a given reaction medium. As such, for any given visible-light photoredox reaction, it is reasonable to assume that only the reaction medium proximal to the vessel wall (i.e., within 2 mm) will experience irradiation.[10] Moreover, as many studies employ the use of directional lamps with cylindrical vials or rounded flasks, a great deal of photonic energy is lost due to reflection (Figure 1). As such, the majority of organic photoredox transformations that have been developed to date are believed to be operating in a "photon-limited" regime as a result of (i) low photon penetration relative to vessel width and (ii) diminished photon capture arising from poor surface area exposure.[11]

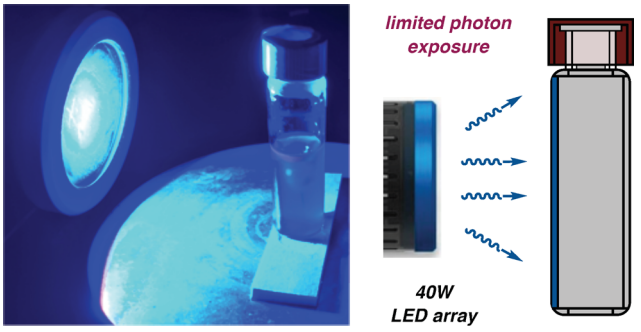

Figure 1. Standard setup with 40 W Kessil blue LEDs and cutaway view to show limited photon exposure.

For any photon-limited regime, it is readily appreciated that an increase in light intensity will lead to a proportional increase in photon-capture events and thereafter the concentration of excited state photocatalyst. As one might imagine, the formation of higher levels of activated photocatalyst will often

Received: April 13, 2017

DOI: 10.1021/acscentsci.7b00159
ACS Cent. Sci. XXXX, XXX, XXX−XXX

lead to improvements in the rates and efficiencies of many elementary catalytic steps, a scenario that can enhance overall reaction times and generally improve efficiencies. With this in mind, many research groups have approached the issue of limited photon penetration via relatively straightforward operational changes, e.g., placing the reaction vessel closer to the light source or increasing the effective light intensity by "numbering-up", wherein multiple lamps are used in combination. Unfortunately, for these cases, the radiant energy from the light source can often result in decreased yields arising from unproductive thermal pathways. Moreover, the introduction of cooling systems to circumvent this problem often results in cumbersome operational protocols (and often without improved performance). During our own studies over the past decade, we have found that the light source, geometry, and distance can significantly alter the reaction efficiency and reaction profile. From our correspondence with other research groups, a general consensus has emerged that a standardized setup for photochemical reactions would likely be broadly adopted, not only to enhance reproducibility but also to aid in the invention or discovery of novel bond-forming reactions. With this in mind, it is important to note that the use of automated flow technologies can provide significant levels of standardization of path length, light intensity, and geometry[12,13] for photocatalysis; however, at the same time this technology is not broadly deployed for small-scale applications across academic, pharmaceutical, fragrance, agrochemical, or materials laboratories.[14]

In this article, we disclose the design of an integrated photoreactor that has been engineered to optimize catalyst photon capture. In an effort to validate both the design and applicability of this system, we have selected eight photocatalytic reactions that are commonly employed in the realm of medicinal chemistry to function as benchmark protocols. Importantly, improved efficiencies and accelerated reaction rates were observed across this range of reaction classes using this new integrated photoreactor.

REACTOR DESIGN

To characterize the total radiant power being delivered to the reaction mixture, we chose a simple analytical technique and a mathematical model based on Newton's law of cooling.[15,16] A rudimentary calorimeter was constructed by embedding a fine thermocouple into a piece of isotropic graphite of the same dimensions as a typical 2 mL reaction mixture in a 2 dram vial. This apparatus allows for the generation of a temperature curve during the testing period, which entails exposing the graphite sample to irradiation for 1 min, followed by a cooling period until the temperature returns to its initial starting point. Using the aforementioned mathematical model (see Supporting Information), the optical power absorbed by the graphite sample was determined by curve fitting. With this model in hand, we constructed and subsequently tested a wide range of LED setups that allow for higher photon capture in comparison to the commonly employed blue LED lamps. In the event, optimum photon capture was observed when the reaction vial was suspended 6 mm above an array of four 3.5 mm square 450 nm XTE LEDs (Cree, Inc., Durham, NC). These LEDs were chosen for their efficiency (>35%), high output (>1.1 W per LED), and a package size readily available in different wavelengths.[17] Notably, while a shorter distance between the LED array and the reaction vessel resulted in higher levels of photon capture, this system suffered from inefficient cooling and issues with reaction temperature control (*vide infra*). As a second critical design element, a tubular mirrored casing was employed to ensure that surface reflected photons could be productively redirected back to the vessel (Figure 2). More

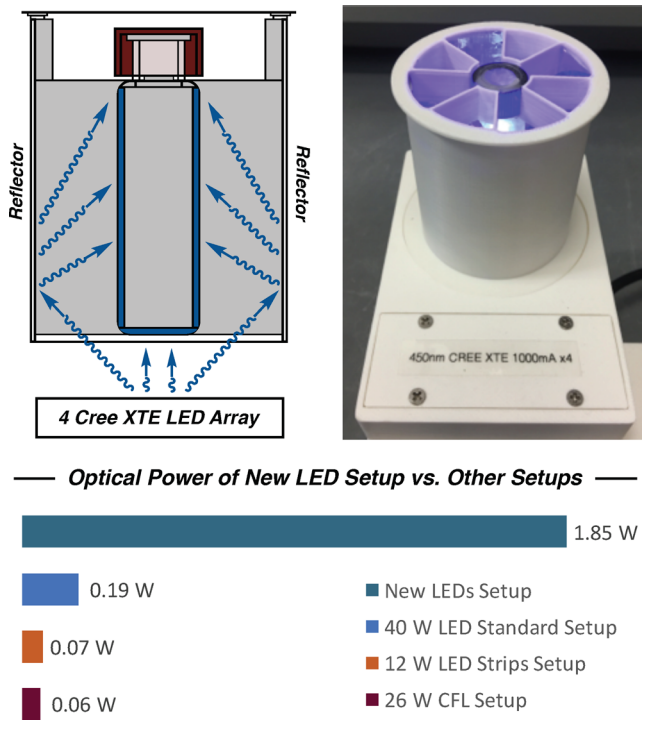

Figure 2. New LED setup with cutaway view to show high photon exposure to the reaction vessel. Comparison with other standard setups showed significant enhancement in optical power.

specifically, the use of this reflective chamber ensures that 360 deg of the vial surface area can be subjected to photon exposure (in contrast to 180 deg via a directed LED lamp). Indeed, calorimeter measurements revealed a 10× increase in total incident radiant power with this XTE system relative to a standard LED Kessil lamp apparatus.[18] With these improvements in hand, this new photon delivery setup was quickly implemented into the design and fabrication of a prototype photoreactor using in-house 3D printing technology.

Our next objective was to engineer an integrated photoreactor that would deliver cooling, stirring, operational simplicity and, most importantly, highly consistent results. With respect to cooling, an axial fan was located underneath the LED array, providing heat extraction for both the reaction vial and the LEDs (Figure 3). This forced convection cooling manifold proved to be simple and highly effective in maintaining reaction temperatures across a broad range (e.g., 25−60 °C) using variable fan speed. As outlined above, the 6 mm vertical gap between the LED array and the reaction vial was found to be optimal for photon capture and minimal thermal flux. For integrated stirring, a brushless motor with a rare-earth magnet was placed immediately underneath the LED array. For operational convenience, the stirring rate and fan speed are controlled via a Raspberry Pi controller with a touchscreen, providing simple management of reaction time and, most significantly, LED power. It is worth noting that this ability to have control of LED power provides an additional reaction parameter for optimization of photoredox protocols (a parameter that is extremely challenging to control with high

DOI: 10.1021/acscentsci.7b00159
ACS Cent. Sci. XXXX, XXX, XXX−XXX

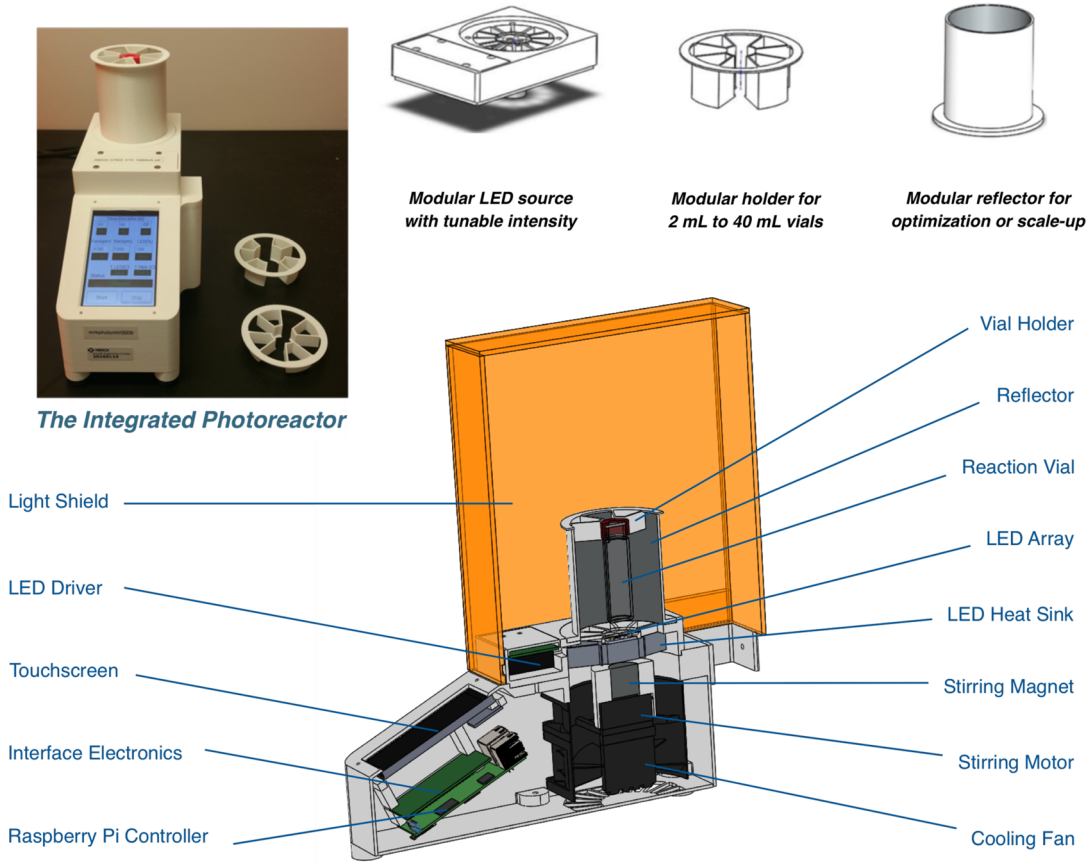

Figure 3. Integrated photoreactor with different modular components, along with labeled cutaway view of the entire device.

accuracy using conventional protocols).[19] Additional design features were included to further expand the capability of the integrated photoreactor. For example, the LED array was built in a pluggable module, allowing users to quickly exchange the irradiation wavelength to best fit the maximum absorbance wavelength of the photocatalyst or sensitizer (Figure 3). A modular vial holder set was designed to accommodate different vial sizes such as 4, 8, 20, and 40 mL vials allowing routine reaction scales from milligram to gram scale. These holders ensure consistent placement while maintaining the optimum vessel-to-LED distance.[20] Finally, the reactor features a light shield and interlock to ensure safe operation that removes user exposure to high-energy visible and UVA light (see Supporting Information).

REACTION COMPARISON

We surveyed the utility of the integrated photoreactor by examining its performance in eight photocatalytic reactions that are commonly employed in medicinal chemistry.

Stephenson Trifluoromethylation. As a calibration point, the trifluoromethylation of 2-acetyl-*N*-Boc pyrrole was performed as originally described by Stephenson et al.[21] This reaction was reproduced in good yield and in an operationally concise time frame (62% yield, 60 min) using a standard LED strip protocol. As shown in Figure 4, when the same transformation was performed using our integrated photoreactor, we were able to achieve the same level of efficiency (64% yield) in a remarkably short reaction time (~3 min).

Li Trifluoromethylation. The recently reported protocol for the trifluoromethylation of aryl rings by the Li group was also investigated.[22] Again, we were able to successfully reproduce the previously reported conditions for the trifluoromethylation of 1,3,5-trimethoxybenzene using a 26 W CFL setup, to afford the desired adduct in 60% yield after 14 h. Using the photoreactor system, we were pleased to observe a 7-fold rate enhancement to generate the trifluoromethylated adduct in 70% yield after only 2 h (Figure 5).

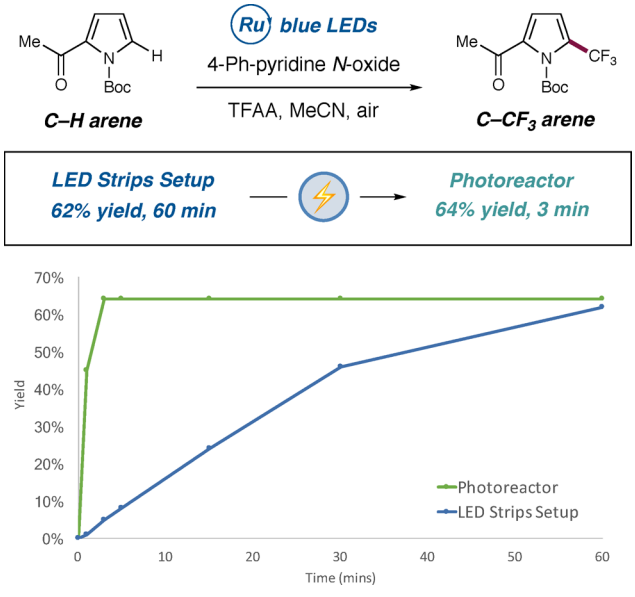

Figure 4. Rate acceleration in the Stephenson trifluoromethylation. Time study performed at 0.80 mmol scale.

DOI: 10.1021/acscentsci.7b00159
ACS Cent. Sci. XXXX, XXX, XXX−XXX

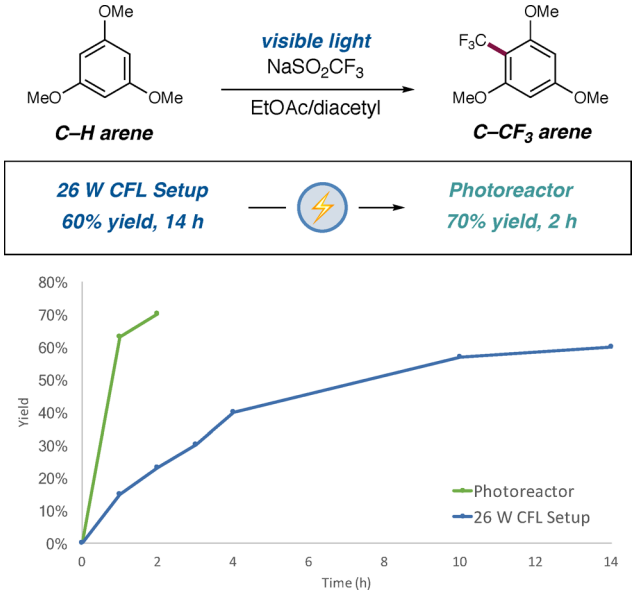

Figure 5. Rate acceleration in the Li trifluoromethylation. Time study performed at 0.25 mmol scale.

Decarboxylative Fluorination. We next examined the capacity of this integrated photoreactor to accelerate transformations that have already been shown to be extremely rapid. As shown in Figure 6, the decarboxylative fluorination of

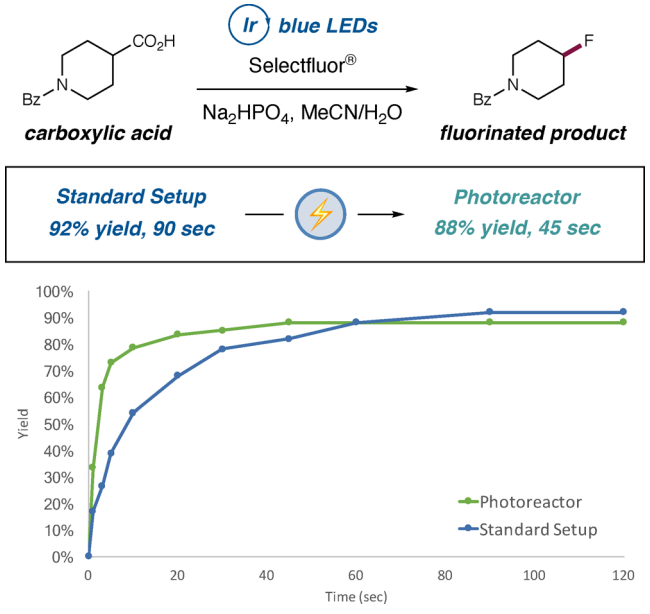

Figure 6. Rate acceleration in decarboxylative fluorination of carboxylic acids. Time study performed at 0.25 mmol scale.

secondary carboxylic acids using standard 40 W blue LEDs proceeded swiftly in excellent yield (92% yield, 90 s).[23] Remarkably, this highly efficient fluorination protocol was accelerated 2-fold using our photoreactor to deliver the desired adduct in only 45 s (88% yield).

We next turned our attention to metallaphotoredox-catalyzed protocols that enable a variety of C–C and C–heteroatom couplings. Given that these transformations are mechanistically founded upon multiple catalytic cycles that must function in concert, we were interested to determine the impact of enhanced photocatalyst excitation.

Molander BF_3K Arylation. In 2014, Molander and coworkers published a seminal manuscript that described the metallaphotoredox-catalyzed coupling of benzyl trifluoroborate salts with aryl halides using nickel catalysis (Figure 7).[24] Under

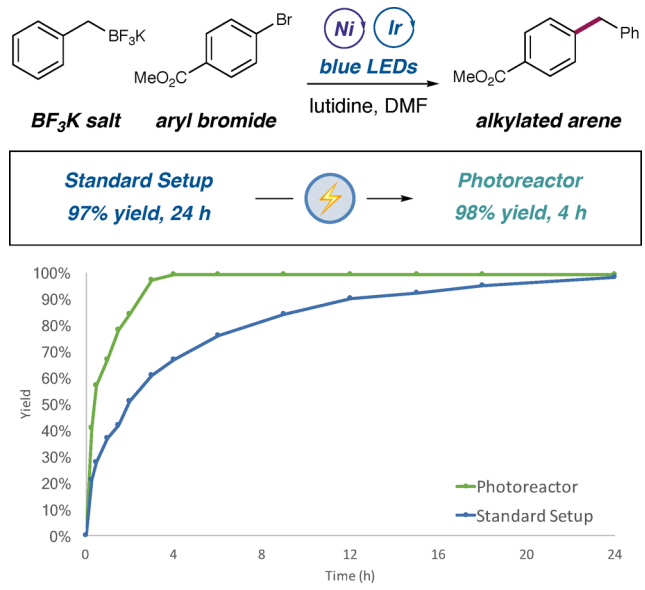

Figure 7. Rate acceleration in coupling with Molander trifluoroborate salts. Time study performed at 0.25 mmol scale.

the standard setup (Kessil lamp 40 W blue LEDs), we were able to successfully reproduce the reported protocol to give the desired alkylation product in 97% yield after 24 h.[25] Remarkably, the integrated photoreactor was able to shorten this reaction time to only 4 h while achieving a comparable yield (98% yield), a net 6-fold rate enhancement.

Decarboxylative Arylation. Using our previously described standard setup (Kessil lamp 40 W blue LEDs), cyclohexane carboxylic acid was converted to the corresponding decarboxylative arylation adduct in good yield (58% yield) over the course of 3 h.[26] When the coupling reaction was performed using the integrated photoreactor, the same transformation was accomplished in superior yield (64% yield) after only 20 min, providing almost an order of magnitude of rate acceleration (Figure 8).

Decarboxylative Alkylation. Good rate acceleration was also observed when the integrated photoreactor was deployed for the decarboxylative alkylation of *N*-Boc-proline.[27] As shown in Figure 9, we observed a nearly 3-fold rate acceleration over the published standard setup, to forge the alkylated pyrrolidine adduct in 9 h (86% yield).

Cross-Electrophile Coupling. The most commonly employed photoredox transformation in the pharmaceutical sector at the present time appears to be the silyl-mediated cross-electrophile coupling reaction (Figure 10).[28,29] As such, we were disappointed to find that our integrated photoreactor exhibited lower efficiency than the reported Kessil lamp based protocol in our initial comparison tests. However, we quickly recognized that the use of the maximum LED output on the photoreactor was promoting a significant increase in reaction rate, that in turn was causing a rapid buildup of deleterious HBr (see Supporting Information). In the case of the reported Kessil

DOI: 10.1021/acscentsci.7b00159
ACS Cent. Sci. XXXX, XXX, XXX−XXX

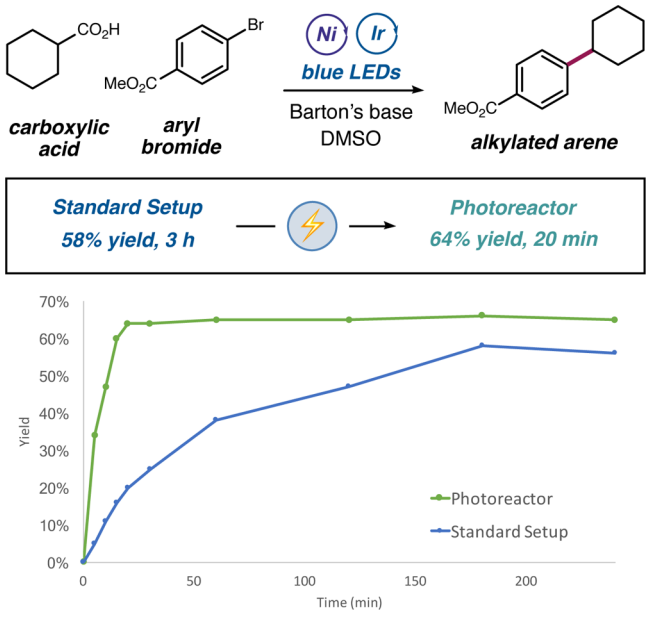

Figure 8. Rate acceleration in decarboxylative arylation. Time study performed at 0.25 mmol scale.

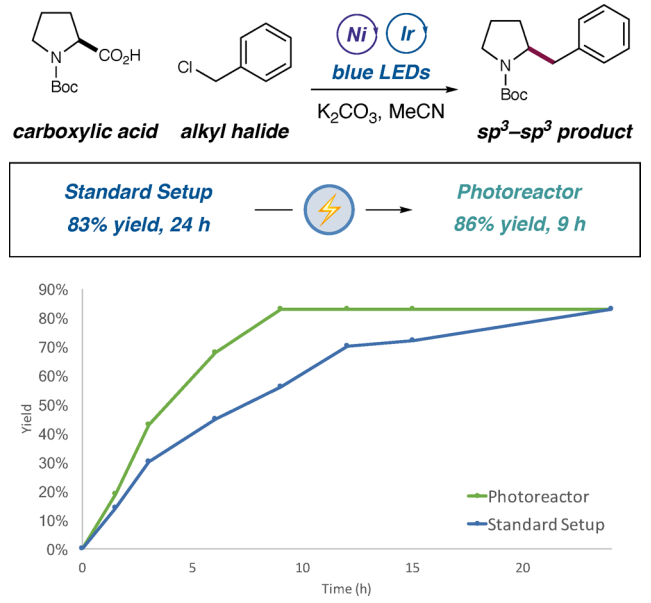

Figure 9. Rate acceleration in decarboxylative alkylation. Time study performed at 0.50 mmol scale.

lamp protocol, the same acid is produced, however, at a rate at which it can be readily neutralized by sodium carbonate, the heterogeneous inorganic base employed. Indeed, when we lowered the photoreactor LED output to 5%, we were able to completely reproduce the original report in terms of time and efficiency. Moreover, in an effort to identify reaction conditions that would allow accelerated reaction times, we subsequently examined a more soluble organic base with the hope that the required neutralization step could be kinetically matched with that of HBr production. Indeed, through the implementation of 2,6-lutidine in lieu of sodium carbonate, the integrated photoreactor could be utilized at full power LED output without loss in efficiency and with a 6-fold enhancement in reaction time (40 min versus 4.5 h). This result serves to reinforce the utility of being able to monitor and implement

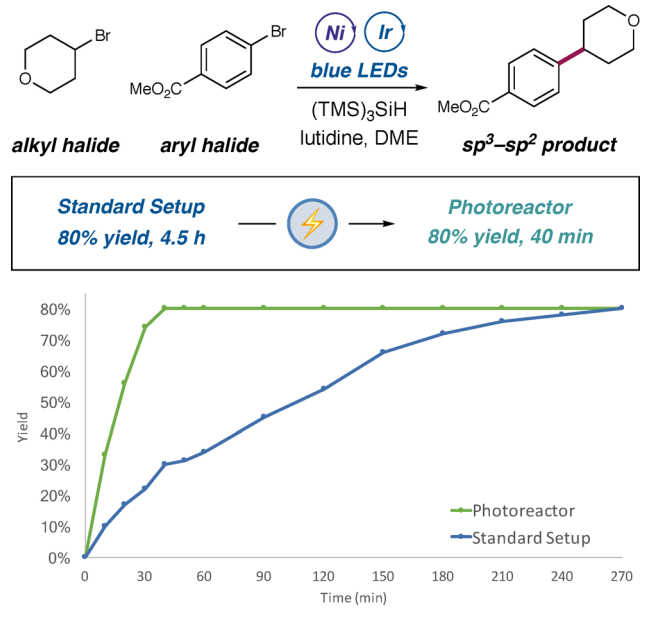

Figure 10. Rate acceleration in cross-electrophile coupling. Time study performed at 0.25 mmol scale.

variable LED intensity with a high level of accuracy and reproducibility, as is possible using the Raspberry Pi interface on this integrated photoreactor.

Photocatalytic C–N Coupling. In addition to C–C bond formation protocols, we also evaluated a metallaphotocatalyzed amination of aryl halides.[30] Using the standard setup with an inexpensive ruthenium photocatalyst (see the Supporting Information) we were able to reproduce the coupling of 4-bromobenzotrifluoride with morpholine in excellent yield in 40 min (Figure 11, 95% yield). Remarkably, by deploying the integrated photoreactor, we observed a 4-fold reduction in reaction time to produce the same amination product in high yield and only 10 min.

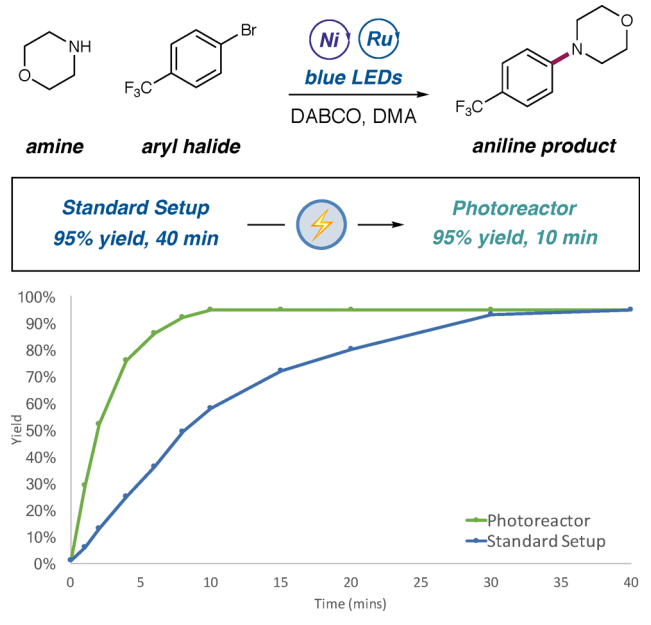

Figure 11. Rate acceleration in amination of aryl halide. Time study performed at 0.25 mmol scale.

DOI: 10.1021/acscentsci.7b00159
ACS Cent. Sci. XXXX, XXX, XXX–XXX

Last, and perhaps most important, we have now validated the utility of the new integrated photoreactor across ten different medicinal chemistry groups located at four different Merck and Co., Inc. research sites in the USA. The successful translation of reaction conditions from previous LED protocols to this standardized photoreactor will be reported in the near future.

CONCLUSIONS

In conclusion, we have designed an integrated small-scale photoreactor that can be employed broadly in the realm of visible-light photocatalysis. The integrated photoreactor enables enhanced light exposure and catalyst excitation across a wide range of photocatalytic reactions and in doing so provides significant rate accelerations in all cases. Indeed, the evaluation of this new reactor in eight photocatalytic transformations that are widely employed in medicinal chemistry settings has confirmed significant performance advantages of this optimized design. Moreover, its successful utilization across multiple research sites highlights its value as a standardized system that enables operational convenience and reproducibility.

ASSOCIATED CONTENT

Supporting Information

The Supporting Information is available free of charge on the ACS Publications website at DOI: 10.1021/acscentsci.7b00159.

Experimental procedures and measurement data for the integrated photoreactor (PDF)

Video demonstrating procedure (MOV)

AUTHOR INFORMATION

Corresponding Authors

*E-mail: dmacmill@princeton.edu.

*E-mail: ian_davies1@merck.com.

ORCID

Chi "Chip" Le: 0000-0002-9614-365X

Author Contributions

‡C.C.L., M.K.W., and Z.-C.S. contributed equally to this work.

Notes

The authors declare no competing financial interest.

ACKNOWLEDGMENTS

Financial support was provided by the NIH NIGMS (R01 GM103558-06) and kind gifts from Merck, Bristol-Myers Squibb, Abbvie, Janssen, and Eli Lilly. We would like to thank the following scientists and engineers at Merck & Co., Inc., and Princeton University for input on reactor design and experimental and technical assistance during preproduction validation of the units. From Princeton University: Patricia Zhang, Megan Shaw, Ryan Evans, Russell Smith, Jack Twilton, and Jack Terrett. From Merck & Co., Inc.: Jack Scott, Shane Krska, Haiqun Tang, Younong Yu, Steve Colletti, Ed Hudak, Kevin Dykstra, Don Henry, Catherine White, David Candito, David Sloman, Min Lu, Sam Kattar, Charles Yeung, Michael VanHeyst, Valerie Shurtleff, Tom Greshock, Jim Perkins, Peter Manley, Abdellatif El Marrouni, Jaume Balsells, Dan DiRocco, Dani Schultz, Andrew Hoover, Sumei Ren, Francois Levesque, Emily Corcoran, John Naber, Matthieu Jouffroy, Prashant Savle, Leo Joyce, Christopher Nawrat, and Steven Oliver.

REFERENCES

(1) Grätzel, M. Artificial photosynthesis: water cleavage into hydrogen and oxygen by visible light. *Acc. Chem. Res.* **1981**, *14*, 376−384.

(2) Meyer, T. J. Chemical approaches to artificial photosynthesis. *Acc. Chem. Res.* **1989**, *22*, 163−170.

(3) Takeda, H.; Ishitani, O. Development of efficient photocatalytic systems for CO_2 reduction using mononuclear and multinuclear metal complexes based on mechanistic studies. *Coord. Chem. Rev.* **2010**, *254*, 346−354.

(4) Kalyanasundaram, K.; Grätzel, M. Applications of functionalized transition metal complexes in photonic and optoelectronic devices. *Coord. Chem. Rev.* **1998**, *177*, 347−414.

(5) Prier, C. K.; Rankic, D. A.; MacMillan, D. W. C. Visible Light Photoredox Catalysis with Transition Metal Complexes: Applications in Organic Synthesis. *Chem. Rev.* **2013**, *113*, 5322−5363.

(6) Shaw, M. H.; Twilton, J.; MacMillan, D. W. C. Photoredox Catalysis in Organic Chemistry. *J. Org. Chem.* **2016**, *81*, 6898−6926.

(7) Staveness, D.; Bosque, I.; Stephenson, C. R. J. Free Radical Chemistry Enabled by Visible Light-Induced Electron Transfer. *Acc. Chem. Res.* **2016**, *49*, 2295−2306.

(8) Romero, N. A.; Nicewicz, D. A. Organic Photoredox Catalysis. *Chem. Rev.* **2016**, *116*, 10075−10166.

(9) Skubi, K. L.; Blum, T. R.; Yoon, T. P. Dual Catalysis Strategies in Photochemical Synthesis. *Chem. Rev.* **2016**, *116*, 10035−10074.

(10) Shvydkiv, O.; Gallagher, S.; Nolan, K.; Oelgemöller, M. From Conventional to Microphotochemistry: Photodecarboxylation Reactions Involving Phthalimides. *Org. Lett.* **2010**, *12*, 5170−5173.

(11) Chu, L.; Lipshultz, J. M.; MacMillan, D. W. C. Merging Photoredox and Nickel Catalysis: The Direct Synthesis of Ketones by the Decarboxylative Arylation of a-Oxo Acids. *Angew. Chem., Int. Ed.* **2015**, *54*, 7929−7933.

(12) Andrews, R. S.; Becker, J. J.; Gagné, M. R. A Photoflow Reactor for the Continuous Photoredox-Mediated Synthesis of *C*-Glycoamino Acids and *C*-Glycolipids. *Angew. Chem., Int. Ed.* **2012**, *51*, 4140−4143.

(13) Tucker, J. W.; Zhang, Y.; Jamison, T. F.; Stephenson, C. R. J. Visible-Light Photoredox Catalysis in Flow. *Angew. Chem., Int. Ed.* **2012**, *51*, 4144−4147.

(14) Elliott, L. D.; Knowles, J. P.; Koovits, P. J.; Maskill, K. G.; Ralph, M. J.; Lejeune, G.; Edwards, L. J.; Robinson, R. I.; Clemens, I. R.; Cox, B.; Pascoe, D. D.; Koch, G.; Eberle, M.; Berry, M. B.; Booker-Milburn, K. I. Batch versus Flow Photochemistry: A Revealing Comparison of Yield and Productivity. *Chem. - Eur. J.* **2014**, *20*, 15226−15232.

(15) Whewell, W. *History of the Inductive Sciences*; Nabu Press: Charleston, 2010.

(16) Burmeister, L. C. *Convective Heat Transfer*, 2nd ed.; Wiley-Interscience: Hoboken, 1993.

(17) Information regarding the Cree XLamp XTE LEDs can be found at www.cree.com.

(18) See the Supporting Information for experimental measurement and comparison of different setups.

(19) Frazier, C. P.; Palmer, L. I.; Samoshin, A. V.; Read de Alaniz, J. Acessing nitrosocarbonyl compounds with temporal and spatial control via the photoredox oxidation of *N*-substituted hydroxylamines. *Tetrahedron Lett.* **2015**, *56*, 3353−3357.

(20) Developments of integrated photoreactor that can hold 6 to 12 reaction vials are underway. The design and results of this study will be reported in due course.

(21) Beatty, J. W.; Douglas, J. J.; Miller, R.; McAtee, R. C.; Stephenson, C. R. J. Photochemical Perfluoroalkylation with Pyridine *N*-Oxides: Mechanistic Insights and Performance on a Kilogram Scale. *Chem* **2016**, *1*, 456−472.

(22) Li, L.; Mu, X.; Liu, W.; Wang, Y.; Mi, Z.; Li, C.-J. Simple and Clean Photoinduced Aromatic Trifluoromethylation Reaction. *J. Am. Chem. Soc.* **2016**, *138*, 5809−5812.

(23) Ventre, S.; Petronijevic, F. R.; MacMillan, D. W. C. Decarboxylative Fluorination of Aliphatic Carboxylic Acids via Photoredox Catalysis. *J. Am. Chem. Soc.* **2015**, *137*, 5654−5657.

DOI: 10.1021/acscentsci.7b00159
ACS Cent. Sci. XXXX, XXX, XXX−XXX

(24) Tellis, J. C.; Primer, D. N.; Molander, G. A. Single-electron transmetalation in organoboron cross-coupling by photoredox/nickel dual catalysis. *Science* **2014**, *345*, 433−436.
(25) Studies were carried out using a modified version of the procedure originally reported by Molander and coworkers: Luo, J.; Zhang, J. Donor-Acceptor Fluorophores for Visible-Light-Promoted Organic Synthesis: Photoredox/Ni Dual Catalytic $C(sp^3)-C(sp^2)$ Cross-Coupling. *ACS Catal.* **2016**, *6*, 873−877.
(26) Zuo, Z.; Ahneman, D. T.; Chu, L.; Terrett, J. A.; Doyle, A. G.; MacMillan, D. W. C. Merging photoredox with nickel catalysis: Coupling of a-carboxyl sp^3-carbons with aryl halides. *Science* **2014**, *345*, 437−440 (The reactivity of cyclohexane carboxylic acid was further optimized in our laboratory).
(27) Johnston, C. P.; Smith, R. T.; Allmendinger, S.; MacMillan, D. W. C. Metallaphotoredox-catalysed sp^3-sp^3 corss-coupling of carboxylic acids with alkyl halides. *Nature* **2016**, *536*, 322−325.
(28) Zhang, P.; Le, C. C.; MacMillan, D. W. C. Silyl Radical Activation of Alkyl Halides in Metallaphotoredox Catalysis: A Unique Pathway for Cross-Electrophile Coupling. *J. Am. Chem. Soc.* **2016**, *138*, 8084−8087.
(29) An informal survey of several pharmaceutical companies in the US has shown that this transformation is most commonly employed for $C_{sp^3}-C_{sp^2}$ coupling at the present time.
(30) Corcoran, E. B.; Pirnot, M. T.; Lin, S.; Dreher, S. D.; DiRocco, D. A.; Davies, I. W.; Buchwald, S. L.; MacMillan, D. W. C. Aryl amination using ligand-free Ni(II) salts and photoredox catalysis. *Science* **2016**, *353*, 279−283.

DOI: 10.1021/acscentsci.7b00159
ACS Cent. Sci. XXXX, XXX, XXX−XXX